Impact of a shearless flow and cylindricity on interchange instability in magnetized plasma

E. S. Benilov
Department of Mathematics, University of Limerick, Limerick, Ireland

(Received 23 August 2004; accepted 16 February 2005; published online 18 April 2005)

The stability of magnetically confined plasmas is sometimes examined using the so-called "slab" model, where the toroidal geometry of the problem is approximated locally by the Cartesian one. In the present paper, a (more accurate) cylindrical approximation is considered and shown to yield results which are qualitatively different from those of the slab model. In particular, if the slab model is applied to the outboard region of the tokamak (where the gradient of the plasma's density and that of the magnetic field are of the same sign), disturbances remain unstable at all times. In the cylindrical model, on the other hand, the $\mathbf{E}\times\mathbf{B}$ flow carries disturbances around the cylinder and they alternate between the unstable and stable regions. Naturally, this reduces the growth rate of instability and makes it dependent on the angular velocity of the flow. © *2005 American Institute of Physics*. [DOI: 10.1063/1.1886830]

I. INTRODUCTION

Interchange instability plays a crucial role in the dynamics of plasma in the outboard region of a tokamak, where the gradient of the plasma density and that of the magnetic field are of opposite signs. The simplest way to examine it is based on the so-called "slab model" (e.g., Refs 1–3), where the toroidal geometry of a tokamak is approximated by the Cartesian one. Then, choosing the region with the maximum density gradient and describing it locally by the slab model, one could expect to reliably calculate the instability's growth rate.

It should be noted, however, that the slab model has two shortcomings. First, the toroidal geometry of the "real" problem implies that the $\mathbf{E}\times\mathbf{B}$ flow does not allow the disturbances to remain in the unstable (outboard) region indefinitely—instead, they alternate between the stable and unstable regions[4] (see Fig. 1). This effect should noticeably weaken the instability, just as it does for ballooning instabilities in toroidal plasma.[5,6] Second, the joint effect of toroidal geometry and nonuniform magnetic field makes the problem inhomogeneous in the poloidal direction—which, in turn, makes disturbances with different poloidal wave numbers interact.

Clearly, the above effects are not described by the Cartesian slab model and, to examine them, one could assume the full toroidal geometry (as has been done in numerous other cases where the Cartesian geometry is insufficient—see, for example, Refs. 5–8). In the present case, however, we can use the simpler cylindrical approximation. Indeed, since the aspect ratio of real tokamaks is large (i.e., the radius of the tokamak torus is much larger than the radius of its cross section), we can approximate the torus by a cylinder.

In the following section of this paper, we shall formulate a cylindrical model of interchange instability and, in Sec. III, examine the structure of steady $\mathbf{E}\times\mathbf{B}$ flows (which can be assumed almost axisymmetric, perturbed by weakly inhomogeneous magnetic field). In Sec. IV, we shall consider the simplest particular case, where the $\mathbf{E}\times\mathbf{B}$ flow, to leading order, corresponds to solid-body rotation. Assuming that the inhomogeneity of the magnetic field is weak, we shall derive a set of linear ordinary differential equations (ODEs) describing the stability of such steady states. Finally, in Sec. V, we shall consider examples where this set can be solved analytically, and compare the results to those of the slab model.

II. THE GOVERNING EQUATIONS

Consider pressure driven interchange motion in a magnetized plasma. Neglecting temperature fluctuations (which will be briefly discussed in Sec. VI), we shall characterize the plasma by the potential ϕ_* and ion concentration n_* (the dimensional variables are marked with asterisks). The corresponding nondimensional variables are

$$\phi = \frac{e}{\mathcal{T}}\phi_*, \quad n = \frac{n_*}{\mathcal{N}} - 1,$$

where e is the elementary charge, and $\mathcal{N}$ and $\mathcal{T}$ are the mean concentration and temperature, respectively. The nondimensional magnetic field, in turn, is given by

$$\mathbf{B} = \frac{\mathbf{B}_*}{\mathcal{B}},$$

where $\mathcal{B}$ is the characteristic value of $|\mathbf{B}_*|$.

Aiming to test the cylindrical approximation of a toroidal plasma, we consider a cross section of the torus (see Fig. 1) and introduce the local Cartesian coordinates (x_*, y_*, z_*), with the z_* axis being perpendicular to the cross section. The corresponding nondimensional coordinates and time are given by

$$(x,y,z) = \frac{(x_*,y_*,z_*)}{\rho}, \quad t = \omega_{ci} t_*,$$

where

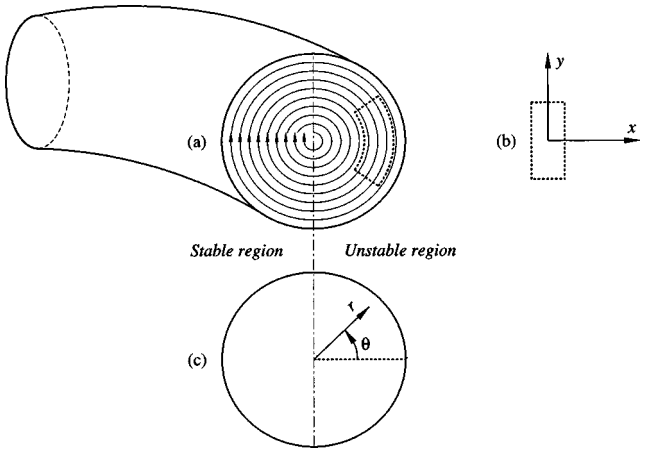

FIG. 1. Formulation of the problem: (a) toroidal model, (b) slab model, and (c) cylindrical model.

$$\rho = \frac{(\mathcal{T}/m_i)^{1/2}}{\omega_{ci}}, \quad \omega_{ci} = \frac{e\mathcal{B}}{m_i},$$

and m_i is the mass of ions.

In what follows, we shall assume that the aspect ratio of the tokamak is large, i.e., radius R of the torus "filled" by plasma is much larger than the radius a of its cross section—in which case the torus can be approximated by a cylinder. Accordingly, within the cross section chosen, the magnetic field can be approximated by a constant value and a weak linear dependence on x, i.e.,

$$\mathbf{B} = (1 - \varepsilon x)\mathbf{z}, \tag{1}$$

where $\mathbf{z}$ is the unit vector directed along the z axis and ε is a small parameter characterizing the decay of the magnetic field with distance from the center of the torus (in terms of the dimensional parameters,

$$\varepsilon = -\frac{\rho\mathcal{B}'}{\mathcal{B}},$$

where $\mathcal{B}'$ is the characteristic gradient of the magnetic field at the cross-section chosen).

We shall also use the flute-mode approximation, i.e., assume that ϕ and n do not depend on the toroidal coordinate—in terms of cylindrical variables, this means that ϕ and n are independent of z. Assuming also that n is small (i.e., n_* is close to its mean value $\mathcal{N}$), we shall describe the plasma's dynamics by the following equations (e.g., Ref. 3):

$$\frac{\partial n}{\partial t} + \{\phi, n\} + K(n - \phi) = 0,$$
$$\frac{\partial \nabla^2\phi}{\partial t} + \{\phi, \nabla^2\phi\} + K(n) = 0, \tag{2}$$

where

$$\nabla^2\phi = \frac{\partial^2\phi}{\partial x^2} + \frac{\partial^2\phi}{\partial y^2}, \quad \{\phi, n\} = \frac{\partial\phi}{\partial x}\frac{\partial n}{\partial y} - \frac{\partial\phi}{\partial y}\frac{\partial n}{\partial x},$$

and the curvature operator K is given by

$$K = -\nabla \cdot \frac{\mathbf{B}\times\nabla}{B^2}.$$

Equations (2) describe coupling of the potential energy of the pressure field to the plasma's kinetic energy, due the curvature of the magnetic field—which gives rise to interchange instability.

Given in Eq. (1), the curvature operator can be reduced to

$$K = \varepsilon\frac{\partial}{\partial y} + O(\varepsilon^2), \tag{3}$$

with ε playing the role of the nondimensional curvature-**B** drift.

Having in mind the cylindrical geometry of the problem, we shall rewrite Eqs. (2) and (3) in terms of polar coordinates (r, θ),

$$r\frac{\partial n}{\partial t} + \frac{\partial\phi}{\partial r}\frac{\partial n}{\partial\theta} - \frac{\partial\phi}{\partial\theta}\frac{\partial n}{\partial r} + \varepsilon\left[\left(\frac{\partial\phi}{\partial r} - \frac{\partial n}{\partial r}\right)r\sin\theta + \left(\frac{\partial\phi}{\partial\theta} - \frac{\partial n}{\partial\theta}\right)\cos\theta\right] = 0, \tag{4}$$

$$r\frac{\partial\nabla^2\phi}{\partial t} + \frac{\partial\phi}{\partial r}\frac{\partial\nabla^2\phi}{\partial\theta} - \frac{\partial\phi}{\partial\theta}\frac{\partial\nabla^2\phi}{\partial r} - \varepsilon\left(\frac{\partial n}{\partial r}r\sin\theta + \frac{\partial n}{\partial\theta}\cos\theta\right) = 0, \tag{5}$$

where

$$\nabla^2\phi = \frac{1}{r}\frac{\partial}{\partial r}\left(r\frac{\partial\phi}{\partial r}\right) + \frac{1}{r^2}\frac{\partial^2\phi}{\partial\theta^2}.$$

Equations (4) and (5) should be supplemented by the usual regularity conditions at the origin,

$$\frac{\partial\phi}{\partial\theta} = 0, \quad \frac{\partial n}{\partial\theta} = 0 \quad \text{at } r = 0, \tag{6}$$

and a condition at the plasma's boundary. Following Ref. 9 (see also Ref. 10), we shall neglect the effect of the scrape-off layer and impose the wall boundary condition,

$$\frac{\partial\phi}{\partial\theta} = 0 \quad \text{at } r = a, \tag{7}$$

where it should be recalled that a is the nondimensional radius of the torus's cross section.

III. STEADY STATES

Assume that the solution does not depend on time,

$$n(r,\theta,t) = N(r,\theta), \quad \phi(r,\theta,t) = \Phi(r,\theta),$$

in which case Eqs. (4) and (5) yield

$$\frac{\partial\Phi}{\partial r}\frac{\partial N}{\partial\theta} - \frac{\partial\Phi}{\partial\theta}\frac{\partial N}{\partial r} + \varepsilon\left[\left(\frac{\partial\Phi}{\partial r} - \frac{\partial N}{\partial r}\right)r\sin\theta + \left(\frac{\partial\Phi}{\partial\theta} - \frac{\partial N}{\partial\theta}\right)\cos\theta\right] = 0, \tag{8}$$

$$\frac{\partial\Phi}{\partial r}\frac{\partial\nabla^2\Phi}{\partial\theta}-\frac{\partial\Phi}{\partial\theta}\frac{\partial\nabla^2\Phi}{\partial r}-\varepsilon\left(\frac{\partial N}{\partial r}r\sin\theta+\frac{\partial N}{\partial\theta}\cos\theta\right)=0. \tag{9}$$

It can be verified by inspection that Eqs. (8) and (9) are consistent with the following ansatz:

$$N(r,\theta)=N^{(0)}(r)+\varepsilon N^{(1)}(r)\cos\theta+\varepsilon^2N^{(2)}(r)\cos 2\theta+\cdots, \tag{10}$$

$$\Phi(r,\theta)=\Phi^{(0)}(r)+\varepsilon\Phi^{(1)}(r)\cos\theta+\varepsilon^2\Phi^{(2)}(r)\cos 2\theta+\cdots, \tag{11}$$

i.e., to leading order, the density and flow are assumed axisymmetric (which agrees with what is observed in real tokamaks—see Ref. 11). Then, substituting Eqs. (10) and (11) into Eqs. (8) and (9), one can show that $N^{(0)}$ and $\Phi^{(0)}$ are arbitrary, whereas $N^{(1)}(r)$ and $\Phi^{(1)}(r)$ satisfy

$$-\frac{d\Phi^{(0)}}{dr}N^{(1)}+\Phi^{(1)}\frac{dN^{(0)}}{dr}+r\left(\frac{d\Phi^{(0)}}{dr}-\frac{dN^{(0)}}{dr}\right)=0,$$

$$-\frac{d\Phi^{(0)}}{dr}\left[\frac{1}{r}\frac{d}{dr}\left(r\frac{d\Phi^{(1)}}{dr}\right)-\frac{1}{r^2}\Phi^{(1)}\right]+\Phi^{(1)}\frac{d}{dr}\left[\frac{1}{r}\frac{d}{dr}(rV)\right]-r\frac{dN^{(0)}}{dr}=0.$$

These equations can be rearranged as follows:

$$VN^{(1)}-\Phi^{(1)}N'=r(V-N'), \tag{12}$$

$$V\Delta_1\Phi^{(1)}-\Phi^{(1)}\Delta_1V=-rN', \tag{13}$$

where

$$V=\frac{d\Phi^{(0)}}{dr},\quad N'=\frac{dN^{(0)}}{dr} \tag{14}$$

are the swirl velocity of the $\mathbf{E}\times\mathbf{B}$ flow and the density gradient respectively, and the operator Δ_1 is

$$\Delta_1=\frac{d^2}{dr^2}+\frac{1}{r}\frac{d}{dr}-\frac{1}{r^2}. \tag{15}$$

The boundary conditions for $N^{(1)}(r)$ and $\Phi^{(1)}(r)$ can be obtained from the general boundary conditions (6) and (7),

$$N^{(1)},\Phi^{(1)}=0\quad\text{at } r=0,a. \tag{16}$$

The boundary-value problem, Eqs. (12), (13), and (16), can be readily solved, i.e., $N^{(1)}$ and $\Phi^{(1)}$ can be related to N' and V—in what follows, however, this solution will not be needed. We shall only consider the following particular case:

$$V=\Omega r, \tag{17}$$

which corresponds to solid-body rotation with angular velocity Ω. In this case, Eq. (13) reduces to

$$\Delta_1\Phi^{(1)}=-\frac{N'}{\Omega}. \tag{18}$$

This identity will be used in the following section.

IV. DISTURBANCES

In what follows, we shall derive an eigenvalue problem describing the stability of steady states with respect to small disturbances. We shall confine ourselves to particular case (17) which corresponds to solid-body rotation, with the density gradient $N'(r)$ still remaining arbitrary. Then, the original two-dimensional (2D) problem will be reduced to a (much simpler) 1D one. Overall, the model based on solid-body rotation allows one to explore the most robust features of cylindrical plasma configurations, whereas more general models will be briefly discussed in Sec. VI.

Note also that, even for case (17), the algebra involved is so cumbersome that nonmathematically minded readers might prefer to jump to the beginning of Sec. IV B, where the asymptotic results are summarized.

A. The linearized stability problem

To examine the stability of a steady state (N,Φ) with respect to small disturbances, we seek a solution in the form

$$n(r,\theta,t)=N(r,\theta)+\tilde{n}(r,\theta,t),$$
$$\phi(x,y,t)=\Phi(r,\theta)+\tilde{\phi}(r,\theta,t), \tag{19}$$

where the tilded variables represent the disturbance. Substituting Eq. (19) into Eqs. (4) and (5) and linearizing the latter, we assume that the disturbance depends in time harmonically,

$$\tilde{n}(r,\theta,t)=\tilde{\tilde{n}}(r,\theta)e^{-i\omega t},\quad \tilde{\phi}(r,\theta,t)=\tilde{\tilde{\phi}}(r,\theta)e^{-i\omega t}$$

and obtain (double tildes omitted)

$$-i\omega rn+\frac{\partial\Phi}{\partial r}\frac{\partial n}{\partial\theta}+\frac{\partial\phi}{\partial r}\frac{\partial N}{\partial\theta}-\frac{\partial\Phi}{\partial\theta}\frac{\partial n}{\partial r}-\frac{\partial\phi}{\partial\theta}\frac{\partial N}{\partial r}+\varepsilon\left[\left(\frac{\partial\phi}{\partial r}-\frac{\partial n}{\partial r}\right)r\sin\theta+\left(\frac{\partial\phi}{\partial\theta}-\frac{\partial n}{\partial\theta}\right)\cos\theta\right]=0, \tag{20}$$

$$-i\omega r\nabla^2\phi+\frac{\partial\Phi}{\partial r}\frac{\partial\nabla^2\phi}{\partial\theta}+\frac{\partial\phi}{\partial r}\frac{\partial\nabla^2\Phi}{\partial\theta}-\frac{\partial\Phi}{\partial\theta}\frac{\partial\nabla^2\phi}{\partial r}-\frac{\partial\phi}{\partial\theta}\frac{\partial\nabla^2\Phi}{\partial r}-\varepsilon\left(\frac{\partial n}{\partial r}r\sin\theta+\frac{\partial n}{\partial\theta}\cos\theta\right)=0. \tag{21}$$

Equations (20) and (21) and boundary conditions (6) and (7) form an eigenvalue problem, where ω is an eigenvalue and (n,ϕ) are the eigenfunctions. If Im $\omega>0$, the disturbance is unstable.

Assuming that ε is a small parameter, we seek a solution in the form

$$n = n^{(0)} + \varepsilon n^{(1)} + \cdots, \quad \phi = \phi^{(0)} + \varepsilon\phi^{(1)} + \cdots,$$

$$\omega = \omega^{(0)} + \varepsilon\omega^{(1)} + \cdots.$$

Recall also that the steady state (N, Φ) is given by expressions (10) and (11). Then, to leading order, Eqs. (20) and (21) yield

$$-i\omega^{(0)} r n^{(0)} + V\frac{\partial n^{(0)}}{\partial\theta} - N'\frac{\partial\phi^{(0)}}{\partial\theta} = 0, \tag{22}$$

$$-i\omega^{(0)} r\nabla^2\phi^{(0)} + V\frac{\partial\nabla^2\phi^{(0)}}{\partial\theta} - \frac{\partial\phi^{(0)}}{\partial\theta}\frac{d}{dr}\left[\frac{1}{r}\frac{d}{dr}(rV)\right] = 0, \tag{23}$$

where V and N' are defined by Eq. (14). In what follows, we shall confine ourselves to particular case (17). Then, the last term in Eq. (23) vanishes, and Eqs. (22) and (23) can be readily solved—assuming that the solution is periodic in θ, we obtain

$$\phi^{(0)}(r,\theta) = 0, \quad n^{(0)}(r,\theta) = n_0^{(0)}(r)e^{ik\theta},$$

$$\omega^{(0)} = k\Omega, \tag{24}$$

where the integer k is the poloidal wave number and $n_0^{(0)}(r)$ is an undetermined function describing the radial structure of the disturbance. Thus, the leading-order frequency turned out to be real (stable)—in fact, expression (24) shows that, to leading order, the disturbance is carried around the cylinder by the flow.

In the next order, Eqs. (20), (21), (10), (11), and (17) yield

$$\Omega r\left(-ik + \frac{\partial}{\partial\theta}\right)n^{(1)} - N'\frac{\partial\phi^{(1)}}{\partial\theta} = i\omega^{(1)} r\, n_0^{(0)} e^{ik\theta} - \left[(\Phi^{(1)} - r)\frac{dn_0^{(0)}}{dr}\sin\theta + \left(\frac{d\Phi^{(1)}}{dr} - 1\right)n_0^{(0)} ik\cos\theta\right]e^{ik\theta}, \tag{25}$$

$$\Omega r\left(-ik + \frac{\partial}{\partial\theta}\right)\nabla^2\phi^{(1)} = \left[\frac{dn_0^{(0)}}{dr} r\sin\theta + n_0^{(0)} ik\cos\theta\right]e^{ik\theta}. \tag{26}$$

We seek a solution in the form

$$\phi^{(1)} = \phi_{+1}^{(1)}(r)e^{i(k+1)\theta} + \phi_0^{(1)}(r)e^{ik\theta} + \phi_{-1}^{(1)}(r)e^{i(k-1)\theta},$$

$$n^{(1)} = n_{+1}^{(1)}(r)e^{i(k+1)\theta} + n_0^{(1)}(r)e^{ik\theta} + n_{-1}^{(1)}(r)e^{i(k-1)\theta},$$

where $\phi_{\pm1,0}^{(1)}(r)$ and $n_{\pm1,0}^{(1)}(r)$ are undetermined functions. Then, Eqs. (25) and (26) yield

$$-\omega^{(1)} n_0^{(0)} - \frac{1}{r}N' k\phi_0^{(1)} = 0, \tag{27}$$

$$\Omega n_{+1}^{(1)} - \frac{1}{r}N'(k+1)\phi_{+1}^{(1)} + \frac{1}{2}\left[\frac{k}{r}\left(\frac{d\Phi^{(1)}}{dr} - 1\right)n_0^{(0)} - \left(\frac{1}{r}\Phi^{(1)} - 1\right)\frac{dn_0^{(0)}}{dr}\right] = 0, \tag{28}$$

$$-\Omega n_{-1}^{(1)} - \frac{1}{r}N'(k-1)\phi_{-1}^{(1)} + \frac{1}{2}\left[\frac{k}{r}\left(\frac{d\Phi^{(1)}}{dr} - 1\right)n_0^{(0)} + \left(\frac{1}{r}\Phi^{(1)} - 1\right)\frac{dn_0^{(0)}}{dr}\right] = 0, \tag{29}$$

$$\Omega\Delta_{k+1}\phi_{+1}^{(1)} + \frac{1}{2}\left(\frac{dn_0^{(0)}}{dr} - \frac{k}{r}n_0^{(0)}\right) = 0, \tag{30}$$

$$-\Omega\Delta_{k-1}\phi_{-1}^{(1)} - \frac{1}{2}\left(\frac{dn_0^{(0)}}{dr} + \frac{k}{r}n_0^{(0)}\right) = 0, \tag{31}$$

where the operator Δ_k is given by

$$\Delta_k = \frac{d^2}{dr^2} + \frac{1}{r}\frac{d}{dr} - \frac{k^2}{r^2}$$

[for $k=1$, this definition coincides with that of Δ_1—see Eq. (15)].

In the next order, we shall need only the equation for ϕ, which can be written in the form

$$\Omega r\left(-ik + \frac{\partial}{\partial\theta}\right)\nabla^2\phi^{(2)} = A_0 e^{ik\theta} + A_{+1}e^{i(k+1)\theta} + A_{-1}e^{i(k-1)\theta} + A_{+2}e^{i(k+2)\theta} + A_{-2}e^{i(k-2)\theta}, \tag{32}$$

where

$$\begin{aligned} A_0 = &-i\omega^{(1)}\Delta_k\phi_0^{(1)} \\ &+ \frac{i}{2}\left(\Phi^{(1)}\frac{d\Delta_{k+1}\phi_{+1}^{(1)}}{dr} - \frac{d\phi_{+1}^{(1)}}{dr}\Delta_1\Phi^{(1)} - r\frac{dn_{+1}^{(1)}}{dr}\right) \\ &+ \frac{i(k+1)}{2}\left(\frac{d\Phi^{(1)}}{dr}\Delta_{k+1}\phi_{-1}^{(1)} - \frac{d\Delta_1\Phi^{(1)}}{dr}\phi_{+1}^{(1)} - n_{+1}^{(1)}\right) \\ &- \frac{i}{2}\left(\Phi^{(1)}\frac{d\Delta_{k-1}\phi_{-1}^{(1)}}{dr} - \frac{d\phi_{-1}^{(1)}}{dr}\Delta_1\Phi^{(1)} - r\frac{dn_{-1}^{(1)}}{dr}\right) \\ &+ \frac{i(k-1)}{2}\left(\frac{d\Phi^{(1)}}{dr}\Delta_{k-1}\phi_{-1}^{(1)} - \frac{d\Delta_1\Phi^{(1)}}{dr}\phi_{-1}^{(1)} - n_{-1}^{(1)}\right) \end{aligned} \tag{33}$$

and the expressions for $A_{\pm1}$ and $A_{\pm2}$ will not be needed. Obviously, Eq. (32) has a solution periodic in θ only if the "resonant" term (the one involving $e^{ik\theta}$) vanishes, i.e.,

$$A_0 = 0. \tag{34}$$

Equations (27)–(31) and (34) form a closed set of ODEs for $n_0^{(0)}$, $n_{\pm1}^{(1)}$, $\phi_0^{(1)}$, $\phi_{\pm1}^{(1)}$.

Observe that some of our equations involve (as a coefficient) the correction $\Phi^{(1)}$ to the steady state, for which we have no explicit expression. It turns out, however, that $\Phi^{(1)}$ can be eliminated.

To do so, use identity (18) to rearrange Eqs. (33) and (34) in the form

$$-2\omega^{(1)}\Omega r\Delta_k\phi_0^{(1)}+k\left(\frac{\Phi^{(1)}}{r}+\frac{d\Phi^{(1)}}{dr}\right)\left(\frac{dn_0^{(0)}}{dr}-\frac{1}{r}n_0^{(0)}\right)$$
$$+N'\left(\frac{d\phi_{+1}^{(1)}}{dr}-\frac{d\phi_{-1}^{(1)}}{dr}\right)+\frac{dN'}{dr}[(k+1)\phi_{+1}^{(1)}$$
$$+(k-1)\phi_{-1}^{(1)}]-\Omega r\frac{d}{dr}(n_{+1}^{(1)}-n_{-1}^{(1)})$$
$$-\Omega[k(n_{+1}^{(1)}+n_{-1}^{(1)})+n_{+1}^{(1)}-n_{-1}^{(1)}]=0. \quad (35)$$

Then, use Eqs. (27)–(29) to eliminate $n_0^{(0)}$, $n_{\pm1}^{(1)}$ from Eqs. (30), (31), and (35). Taking into account, where necessary, Eqs. (18), we obtain a closed set for $\phi_0^{(1)}$, $\phi_{\pm1}^{(1)}$:

$$\frac{2\Omega\omega^{(1)}}{k}\frac{r^2}{N'}\Delta_k\phi_0^{(1)}-\frac{2kN'}{2\Omega\omega^{(1)}}\phi_0^{(1)}+r\frac{d}{dr}(\phi_{+1}^{(1)}+\phi_{-1}^{(1)})$$
$$+(k+1)\phi_{+1}^{(1)}-(k-1)\phi_{-1}^{(1)}=0, \quad (36)$$

$$\frac{2\Omega\omega^{(1)}}{k}\Delta_{k+1}\phi_{+1}^{(1)}-\frac{d}{dr}\left(\frac{N'\phi_0^{(1)}}{r}\right)+\frac{k}{r^2}N'\phi_0^{(1)}=0, \quad (37)$$

$$\frac{2\Omega\omega^{(1)}}{k}\Delta_{k-1}\phi_{-1}^{(1)}-\frac{d}{dr}\left(\frac{N'\phi_0^{(1)}}{r}\right)-\frac{k}{r^2}N'\phi_0^{(1)}=0. \quad (38)$$

Note that Eqs. (36)–(38) involve only the leading-order parameters of the steady state (N' and Ω)—i.e., $\Phi^{(1)}$ has been eliminated.

The boundary conditions for $\phi_0^{(1)}$ and $\phi_{\pm1}^{(1)}$ follow from the original boundary conditions (6) and (7),

$$\phi_0^{(1)},\phi_{\pm1}^{(1)}=0 \quad \text{at } r=0,a. \quad (39)$$

The asymptotic eigenvalue problem, Eqs. (36)–(39), involves functions of a single variable and is, therefore, much simpler than the two-dimensional original problem, Eqs. (20), (21), (6), and (7).

B. Summary of the asymptotic results

Thus, we have examined a problem, Eqs. (20) and (21) and (6), (7), which describes the stability of a steady state with potential $\Phi(r,\theta)$ and density $N(r,\theta)$ with respect to linear harmonic disturbances. Since the inhomogeneity of the magnetic field is weak, the functions $\Phi(r,\theta)$ and $N(r,\theta)$ are almost axisymmetric,

$$\Phi(r,\theta)=\Phi^{(0)}(r)+O(\varepsilon), \quad N(r,\theta)=N^{(0)}(r)+O(\varepsilon),$$

and we have also assumed that, to leading order, the plasma rotates as a solid,

$$\Phi^{(0)}=\frac{1}{2}\Omega r^2,$$

where Ω is the angular frequency.

In this case, the density variation induced by the disturbance has the form

$$\tilde{n}(\theta,r,t)=n_0^{(0)}(r)e^{ik\theta-i\omega t}+O(\varepsilon), \quad (40)$$

where ω and k are the frequency and poloidal wave numbers, and $n_0^{(0)}(r)$ describes the disturbance's radial structure; the frequency of the disturbance is given by

$$\omega=\Omega k+\varepsilon\omega^{(1)}+O(\varepsilon^2) \quad (41)$$

(i.e., if $\mathrm{Im}\,\omega^{(1)}>0$, the disturbance is unstable); the disturbance-induced variation of the potential is

$$\tilde{\phi}(\theta,r,t)=\varepsilon[\phi_{+1}^{(1)}(r)e^{i(k+1)\theta}+\phi_0^{(1)}(r)e^{ik\theta}+\phi_{-1}^{(1)}$$
$$\times(r)e^{i(k-1)\theta}]e^{-i\omega t}+O(\varepsilon^2), \quad (42)$$

where $\phi_0^{(1)}$ is related to the disturbance-induced density variations by

$$n_0^{(0)}(r)=-\frac{k}{\omega^{(1)}r}\phi_0^{(1)}(r). \quad (43)$$

Finally, the functions $\phi_0(r)$, $\phi_{\pm1}(r)$ and the first-order frequency $\omega^{(1)}$ satisfy eigenvalue problem, Eqs. (36)–(39), where

$$N'(r)=\frac{dN^{(0)}}{dr}$$

is the steady state's density gradient.

Thus, the eigenvalue of problem (36)–(39) determines the stability properties of the steady state [through formulas (41)], and the eigenfunctions determine the spatial structure of the disturbance [through formulas (40), (42), and (43)].

Before we proceed, rewrite Eqs. (36)–(39) in terms of new variables,

$$\phi_{+1}=c\phi_{+1}^{(1)}, \quad \phi_{-1}=c\phi_{-1}^{(1)}, \quad \phi_0=\frac{N'}{r}\phi_0^{(1)}, \quad (44)$$

where

$$c=\frac{2\Omega\omega^{(1)}}{k}. \quad (45)$$

Substitution of Eq. (44) into Eqs. (36)–(38) yields

$$\frac{c^2r}{N'}\Delta_k\left(\frac{r\phi_0}{N'}\right)-2\phi_0+\frac{d}{dr}(\phi_{+1}+\phi_{-1})+\frac{k+1}{r}\phi_{+1}$$
$$-\frac{k-1}{r}\phi_{-1}=0, \quad (46)$$

$$r\Delta_{k+1}\phi_{+1}=r\frac{d\phi_0}{dr}-k\phi_0, \quad (47)$$

$$r\Delta_{k-1}\phi_{-1}=r\frac{d\phi_0}{dr}+k\phi_0, \quad (48)$$

$$\phi_0,\phi_{\pm1}=0 \quad \text{at } r=0,a. \quad (49)$$

V. EXAMPLES

First of all, observe that $\omega^{(1)}$ does not appear in problems (46)–(49) by itself, but only in combination with Ω [see Eq. (45)]—hence, the growth rate, $\mathrm{Im}\,\omega^{(1)}$, is a reciprocal of the angular velocity Ω of the (rotational) $\mathbf{E}\times\mathbf{B}$ flow. It should be emphasized that weakening of interchange instability due to a nonsheared flow is *not* described by the slab model.

Note also that, in addition to the main harmonic ϕ_0, problems (46)–(49) involve the sideband harmonics $\phi_{\pm1}$. To find out how these effect the stability, consider

$$\int_0^a [r\phi_0^*(46) - \phi_{+1}(47)^* - \phi_{-1}(48)^*]dr,$$

where the asterisk denotes complex conjugate. After straightforward algebra involving integration by parts and the use of boundary conditions (49), we obtain

$$c^2\int_0^a \left[r\left|\frac{d}{dr}\left(\frac{r\phi_0}{N'}\right)\right|^2 + \frac{k^2}{r}\left|\frac{r\phi_0}{N'}\right|^2\right]dr$$
$$= \int_0^a \left\{ -2r|\phi_0|^2 + r\left(\left|\frac{d\phi_{+1}}{dr}\right|^2 + \left|\frac{d\phi_{-1}}{dr}\right|^2\right) + \frac{1}{r}[(k+1)^2|\phi_{+1}|^2 + (k-1)^2|\phi_{-1}|^2]\right\}dr.$$

This identity shows that the contribution of the main harmonic ϕ_0 to c^2 is negative (destabilizing), whereas $\phi_{\pm1}$ act in the opposite (stabilizing) manner. It remains to be seen, however, whether the sideband harmonics can stabilize the plasma completely.

Before examining this question, rewrite Eqs. (46)–(49) in a more convenient form. Observe that Eq. (46) can be rearranged as

$$\frac{c^2 r}{N'}\Delta_k\left(\frac{r\phi_0}{N'}\right) + 2\chi = 0, \tag{50}$$

where

$$2\chi = \frac{d\phi_{+1}}{dr} + \frac{d\phi_{-1}}{dr} + \frac{k+1}{r}\phi_{+1} - \frac{k-1}{r}\phi_{-1} - 2\phi_0. \tag{51}$$

Then, it can be verified by inspection that

$$\Delta_k\chi = 0. \tag{52}$$

In what follows, it is convenient to treat χ as an additional unknown—thus, we shall need two boundary conditions for it. In order to find the one at $r=0$, observe that Eq. (52) implies

$$\chi = \text{const}_1 r^k + \text{const}_2 r^{-k}.$$

Hence, to guarantee that χ is finite, we can simply require that

$$\chi = 0 \quad \text{at } r = 0. \tag{53}$$

To derive a condition at the boundary of the plasma, in turn, we shall use χ's definition (51) and the boundary conditions (49) for the other variables—which yields

$$2\chi = \frac{d\phi_{+1}}{dr} + \frac{d\phi_{-1}}{dr} \quad \text{at } r = a. \tag{54}$$

From now on, our eigenvalue problem will consist of Eqs. (47), (48), (50), and (52) and boundary conditions (49), (53), and (54).

A. An example: Parabolic density profile

Consider a particular case, where the leading-order density $N^{(0)}$ depends on r parabolically—in terms of N', this corresponds to

$$N'(r) = N''r, \tag{55}$$

where N'' is a constant. Then, eigenvalue problem, Eqs. (47), (48), (50), (52), (49), (53), and (54), can be solved exactly and yields the following expressions for the eigenfunctions:

$$\chi = Ar^k, \quad \phi_0 = \frac{AN''^2 r^k(a^2 - r^2)}{2(k+1)c^2},$$
$$\phi_{+1} = -\frac{AN''^2 r^{k+1}(r^2 - a^2)}{4(k+1)(k+2)c^2}, \quad \phi_{-1} = -\frac{AN''^2 r^{k-1}(r^2 - a^2)^2}{8(k+1)c^2}, \tag{56}$$

where A is a constant of integration. The eigenvalue, in turn, is

$$c^2 = -\frac{(N''a)^2}{4(k+2)(k+1)},$$

which, after we take into account Eq. (45), yields the following nondimensional growth rate:

$$\text{Im}\,\omega \approx \varepsilon\,\text{Im}\,\omega^{(1)} = \frac{\varepsilon k}{4\sqrt{(k+2)(k+1)}}\left|\frac{N''a}{\Omega}\right|. \tag{57}$$

This formula is illustrated in Fig. 2(a)—one can see that the growth rate increases with k, i.e., towards the short-wave end of the spectrum.

B. An example: Short disturbances (large k)

As suggested by the previous example, much of the growth occurs at small wavelengths. Therefore, it is interesting to examine the $(k\to\infty)$ limit of eigenvalue problems, Eqs. (47), (48), (50), (52), (49), (53), and (54).

To do so, solve Eq. (52) for χ,

$$\chi = Ar^k, \tag{58}$$

where A is a constant of integration, and introduce new variables, $\hat\phi_0$, $\hat\phi_{\pm1}$, $\hat c$, such that

$$\phi_0 = kr^k\hat\phi_0, \quad \phi_{+1} = r^{k+1}\hat\phi_{+1}, \quad \phi_{-1} = kr^{k-1}\hat\phi_{-1}, \tag{59}$$

$$c = k^{-1}\hat c. \tag{60}$$

Then, substituting Eqs. (58)–(60) into problems, Eqs. (47), (48), (50), (49), (53), and (54) and keeping leading-order terms only, we obtain

$$\frac{2\hat c^2 r}{N'}\frac{d}{dr}\left(\frac{r\hat\phi_0}{N'}\right) + 2Ar = 0, \quad 2\frac{d\hat\phi_{+1}}{dr} = \frac{d\hat\phi_0}{dr},$$
$$\frac{d\hat\phi_{-1}}{dr} = r^2\hat\phi_0. \tag{61}$$

$$r^k\hat\phi_0, r^{k+1}\hat\phi_{+1}, r^{k-1}\hat\phi_{-1} \to 0 \quad \text{as } r \to 0, \tag{62}$$

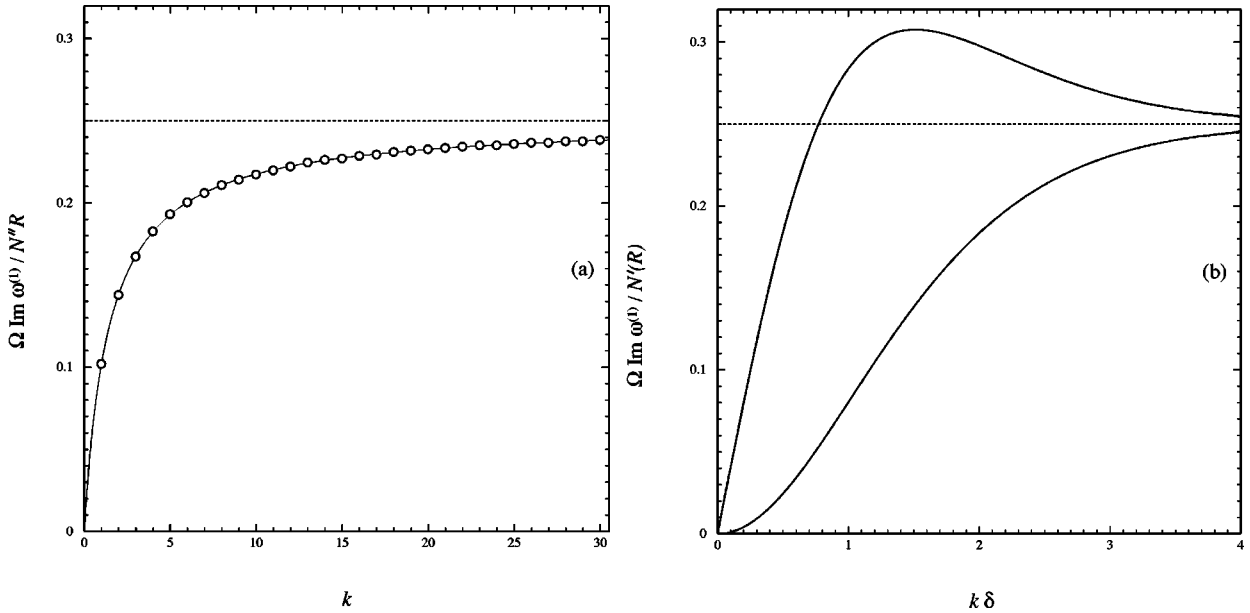

FIG. 2. The nondimensional growth rate Im $\omega^{(1)}$ vs poloidal wave number k (the dotted line shows the limiting growth rate as $k\to\infty$). (a) The case of parabolic density profile (55); (b) the narrow annulus model (δ is the ratio of the half-width and radius of the annulus).

$$\hat{\phi}_0 = \hat{\phi}_{+1} = \hat{\phi}_{-1} = 0, \quad 2A = a\frac{d\hat{\phi}_{+1}}{dr} + \frac{1}{a}\frac{d\hat{\phi}_{-1}}{dr} \quad \text{at } r = a. \tag{63}$$

The simplified eigenvalue problem, Eqs. (61) and (63), can be readily solved for arbitrary $N'(r)$, resulting in

$$\hat{c}^2 = -\frac{1}{4}N'(a).$$

Backtracking substitutions (45) and (60), we obtain the following expression for the nondimensional growth rate:

$$\text{Im } \omega \approx \varepsilon \text{ Im } \omega^{(1)} = \frac{\varepsilon}{4}\left|\frac{N'(a)}{\Omega}\right|; \tag{64}$$

interestingly, it is fully determined by the boundary value of the density gradient $N'(r)$. It should also be mentioned that Eq. (64) agrees with the $k\to\infty$ limit of formula (57) obtained for the parabolic $N^{(0)}(r)$.

In order to compare the cylindrical and slab models, note that the slab-model equivalent of formula (64) is

$$\text{Im } \omega \approx \sqrt{\varepsilon N'_{\max}}, \tag{65}$$

where $N'_{\max}$ is the maximum density gradient. There are two differences between Eqs. (64) and (65). First, the latter is independent of Ω (simply because the slab model is not affected by shearless flows). Second, Eq. (64) scales with ε, whereas Eq. (65) scales with $\varepsilon^{1/2}$—i.e., the latter is much larger than the former. The difference in orders is a result of averaging over stable/unstable regions which has been carried out when obtaining Eq. (64).

Finally, note that the applicability of formula (64) is limited by dissipation (which affects small scales).

C. An example: A narrow annulus

Assume that the plasma is confined to an annulus formed by two concentric cylinders of radii $a\pm\Delta a$. Such configuration is the closest cylindrical analog of the slab model and will allow one to make a more meaningful comparison with it.

In this case, both boundary conditions should be of the no-flow type,

$$\phi_0, \phi_{\pm1} = 0, \quad 2\chi = \frac{d\phi_{+1}}{dr} + \frac{d\phi_{-1}}{dr} \quad \text{at } r = a(1\pm\delta), \tag{66}$$

where

$$\delta = \frac{\Delta a}{a}.$$

Then, to make the (cylindrical) annulus as similar as possible to a "slab," we assume the former to be narrow, i.e.,

$$\delta \ll 1.$$

We shall also assume that the density gradient N' does not change much across the annulus, i.e., simply put

$$N'(r) = N' = \text{const}.$$

To take advantage of the smallness of δ, introduce the following scaled variables:

$$\hat{r} = \frac{r-a}{a\delta}, \quad \hat{\phi}_0 = \phi_0, \quad \hat{\chi} = \chi, \quad \hat{\phi}_{\pm1} = \frac{\phi_\pm}{a\delta},$$

$$\hat{k} = \delta k, \quad \hat{c} = \frac{c}{\delta}.$$

Observe that the scaling of k implies $k\sim\delta^{-1}$—which, in fact, includes $k\ll\delta^{-1}$ and $k\gg\delta^{-1}$ as limiting cases.

Rewriting problems, Eqs. (47), (48), (50), (52), and (66), in terms of the new variables and keeping the leading-order terms only, we obtain

$$\frac{\hat{c}^2}{N'^2}\left(\frac{d^2\hat{\phi}_0}{d\hat{r}^2}-k^2\hat{\phi}_0\right)+2\chi=0, \quad \frac{d^2\hat{\chi}}{d\hat{r}^2}-k^2\hat{\chi}=0, \tag{67}$$

$$\frac{d^2\hat{\phi}_{+1}}{d\hat{r}^2}-k^2\hat{\phi}_{+1}=\frac{d\hat{\phi}_0}{d\hat{r}}-k\hat{\phi}_0,$$

$$\frac{d^2\hat{\phi}_{-1}}{d\hat{r}^2}-k^2\hat{\phi}_{-1}=\frac{d\hat{\phi}_0}{d\hat{r}}+k\hat{\phi}_0, \tag{68}$$

$$\hat{\phi}_0,\hat{\phi}_{\pm1}=0, \quad 2\hat{\chi}=\frac{d\hat{\phi}_{+1}}{d\hat{r}}+\frac{d\hat{\phi}_{-1}}{d\hat{r}} \quad \text{at } \hat{r}=\pm1. \tag{69}$$

Observe that Eqs. (67) and (68) are linear ODEs with constant coefficients—hence, they can be readily solved. The resulting dispersion relation is a biquadratic equation for $\hat{c}$ with two unstable and two stable solutions. The coefficients of this equation are extremely bulky, and we shall not present them here—instead, its solution (growth rate versus poloidal wave number) is plotted in Fig. 2(b). One can see that, unlike the previous cases, the most unstable disturbance has a finite wavelength (it is comparable to the width of the annulus).

Finally, when comparing the slab model with cylindrical annulus, observe that the former has infinitely many modes, whereas the latter has only two modes (one of these has odd, and the other one even, spatial structure). In addition, the growth rate of instability in a cylindrical annulus decreases with the angular velocity Ω (as mentioned before), whereas the slab model simply does not involve Ω, or any other parameter analogous to it. A similar effect has been observed in Ref. 12: shearless flows weaken the instability of ion temperature gradient modes in toroidal and helical configurations, but not in the slab one.

VI. CONCLUDING REMARKS

Thus, we have examined the effect of cylindricity on interchange instability in a magnetized plasma. Assuming that the flow is close to axisymmetric, we calculated the instability's parameters and compared them to those calculated through the so-called slab (Cartesian) model.

First, if the latter is applied to the outboard region of the tokamak (where the gradient of the plasma's density and that of the magnetic field are of the same sign), disturbances remain unstable at all times. In the cylindrical model, on the other hand, the $\mathbf{E}\times\mathbf{B}$ flow carries disturbances around the cylinder, and they alternate between the unstable and stable regions. Naturally, this effect weakens the instability, and also makes its growth rate scale with Ω^{-1}, where Ω is the angular velocity of the $\mathbf{E}\times\mathbf{B}$ flow. Second, in the cylindrical model, the main harmonic (with a poloidal wave number k) interacts with the sideband waves (with poloidal wave numbers $k\pm1$), and this interaction is also of stabilizing nature—however, in all cases considered, plasma would not become *completely* stable.

Note also that all results of this paper are based on a particular case of the $\mathbf{E}\times\mathbf{B}$ flow, such that, to leading order, the plasma rotates as a solid. This example allows one to explore the most robust features of cylindrical plasma configurations, but it will need to be generalized before a comparison with real plasmas could be made. Such generalization, however, is not straightforward—mainly because the inhomogeneity of the magnetic field (which causes the interchange instability) is weak. To illustrate the mathematical implications of this fact, consider an $\mathbf{E}\times\mathbf{B}$ flow of a "general" profile $V(r)$ and observe that the leading-order equation (23) coincides with a similar equation in 2D hydrodynamics. Then, generally, it has either *unstable solutions*, or *no solutions* at all—as a result, interchange instability is either much weaker than the leading-order hydrodynamic instability, or simply does not exist. In fact, exchange instability exists only if the leading-order equation (23) has a *neutrally stable* solution (which would become unstable in next orders, were the magnetic field be taken into account)—this is what happens in the case of rotation as a solid examined here.

Apart from this particular case, there seems to be only two instances, where the leading-order problem may have neutrally stable solutions.

(1) Assume that the profile of an $\mathbf{E}\times\mathbf{B}$ flow is almost linear, but with a small correction,

$$V(r)=\Omega r+\varepsilon^2V^{(2)}(r).$$

Then, the leading-order problem should remain as in this paper, whereas $V^{(2)}(r)$ will appear in a modified version of the asymptotic equations (46)–(48). In other words, even small deviation from rotation as a solid may affect strongly the stability of plasma.

(2) Another less obvious example arises in cases where $V(r)$ has a maximum. As shown for similar problems,[13,14] extrema of the velocity profile can capture disturbances (both stable and unstable). Note also that local maxima of the radial electric filed (and, consequently, those of the poloidal motion) have indeed been observed experimentally (see Ref. 15).

Finally, the present results can be extended to include temperature variations. It should be noted, however, that the equation governing temperature is very much similar to that governing density, and we expect that the temperature effects will not change the results too much.

[1] A. B. Hassam, Phys. Plasmas **6**, 3882 (1999).
[2] P. W. Terry, Rev. Mod. Phys. **72**, 109 (2000).
[3] V. Naulin, J. Nycander, and J. Juul Rasmussen, Phys. Plasmas **10**, 1075 (2003).
[4] Another mechanism connecting the stable and unstable regions is based on the motion of particles along the magnetic field lines (which are helices on nested tori). This mechanism will not be examined in this paper.
[5] F. L. Waelbroeck and L. Chen, Phys. Fluids B **3**, 601 (1991).
[6] R. L. Miller, F. L. Waelbroeck, A. B. Hassam, and R. E. Waltz, Phys. Plasmas **2**, 3676 (1995).
[7] J. W. Connor, R. J. Hastie, and J. B. Taylor, Proc. R. Soc. London, Ser. A **365**, 1 (1979).
[8] J. W. Connor, J. B. Taylor, and H. R. Wilson, Phys. Rev. Lett. **70**, 1803 (1993).
[9] D. C. Montgomery, Phys. Plasmas **7**, 4785 (2000).

[10]P. W. Terry, Phys. Plasmas **7**, 4787 (2000).
[11]K. H. Burrell, Phys. Plasmas **4**, 1499 (1997).
[12]L. Villard, A. Bottino, O. Sauter, and J. Vaclavik, Phys. Plasmas **9**, 2684 (2002).
[13]E. S. Benilov, V. Naulin, and J. Juul Rasmussen, Phys. Fluids **14**, 1674 (2002).
[14]E. S. Benilov, Phys. Fluids **15**, 718 (2003).
[15]P. Zhu, W. Horton, and H. Sugama, Phys. Plasmas **6**, 2503 (1999).